Applied Chemical Engineering (2025) Volume 8 Issue 4 ISSN: 2578-2010 (O)
doi: 10.59429/ace.v8i4.5755

ORIGINAL RESEARCH ARTICLE

XPS-Based Chemical Mapping of Interfacial Bonding in FDM-AM Polymer Surfaces

Smai ail salam[1] , Mohammed Fadhil Abbood[2] , Sarah salam Ali[1], Hayder Hamid Abbas Al-Anbari[3], Muntadher Abed Hussein[4], Fakhri Alajeeli[5], Ameer Hassan Idan[6,*], Hayder Abdulhasan Hammoodi[7] , Sanan Thaer Abdalwahab[8]

[1] *Department of Analytics Laboratories, Al-Farahidi University, Baghdad, 10111,Iraq*
[2] *Legal Affairs Department, Iraqia University,Baghdad,10111,Iraq*
[3] *College of Pharmacy, Ahl Al-Bayt University, Kerbala,13004, Iraq*
[4] *Al-Manara College For Medical Sciences,University of Manara, Amarah, Maysan, 62001,Iraq*
[5] *Department of Medicinal Chemistry, Al-Hadi University College, Baghdad, 10011, Iraq*
[6] *Department of Medicinal Chemistry, Al-Zahrawi University College, Karbala,56001, Iraq*
[7] *Department of Dentistry, Mazaya University College, Dhi Qar,21974, Iraq*
[8] *Microbiology, Clinical Immunology, Al-Turath University, Baghdad, 10013, Iraq*
***Corresponding author:** Ameer Hassan Idan, Haibethassan96@gmail.com

ABSTRACT

Fused Deposition Modeling (FDM), a widely adopted additive manufacturing (AM) process for polymers, often suffers from weak interfacial bonding between printed layers, which limits the mechanical reliability of fabricated components. In this work, X-ray Photoelectron Spectroscopy (XPS) was employed as a surface-sensitive analytical technique to chemically map the interfacial regions of FDM-processed polymer specimens. By correlating elemental distributions and chemical states with print-layer orientation, the study reveals distinct interfacial bonding characteristics that govern adhesion at the microscale. High-resolution chemical mapping demonstrates the presence of oxidative species, chain scission fragments, and thermally induced chemical rearrangements localized at interlayer boundaries. These findings provide new insights into the chemical origin of bonding heterogeneity in FDM-AM polymers and highlight XPS as a powerful diagnostic tool for guiding surface modification strategies to enhance interfacial adhesion. The approach establishes a framework for linking interfacial chemistry to mechanical performance, ultimately advancing the design of more reliable polymer-based additive manufacturing applications.

Keywords: X-ray Photoelectron Spectroscopy (XPS); Fused Deposition Modeling (FDM); Additive Manufacturing (AM); Polymer Interfaces; Interfacial Bonding; Surface Chemistry; Chemical Mapping; Layer Adhesion

ARTICLE INFO

Received: 25 August 2025
Accepted: 01 December 2025
Available online: 11 December 2025

1. Introduction

Additive manufacturing (AM) of polymers, particularly through fused deposition modeling (FDM), has emerged as one of the most transformative technologies enabling the rapid production of customized, lightweight, and complex structures with reduced material waste compared to conventional subtractive techniques [1-3]. FDM, also known as material extrusion (MEX), fabricates components by extruding thermoplastic filaments through a heated nozzle and depositing them layer by layer to build up a three-dimensional structure [4-6]. While this approach offers substantial advantages in terms of flexibility, cost-effectiveness, and accessibility,

a well-recognized limitation lies in the mechanical anisotropy of printed parts, largely dictated by weak interfacial adhesion between adjacent layers [7-9]. The strength of FDM parts is often inferior along the build direction compared to the in-plane orientation, a phenomenon directly linked to insufficient bonding at polymer interfaces, where incomplete interdiffusion, chain entanglement, and chemical heterogeneity hinder the formation of robust interlayer welds [10-12]. The state of the art in FDM research has therefore placed increasing emphasis on understanding the mechanisms of interfacial bonding, exploring strategies to improve adhesion, and developing advanced characterization techniques capable of resolving surface and subsurface chemistry at these critical regions [13-15]. Previous studies have investigated interfacial bonding primarily from a mechanical or thermal standpoint, analyzing the effect of process parameters such as nozzle temperature [16], raster angle [17], layer thickness [18], build orientation[19], and cooling rate on weld strength [20]. Thermal models have described interdiffusion of polymer chains across interfaces using reptation theory, while molecular dynamics simulations have provided atomistic insights into entanglement density and healing kinetics [21-23]. Experimental approaches including optical microscopy, atomic force microscopy, and scanning electron microscopy have revealed morphological signatures of incomplete fusion, while mechanical testing methods such as peel, lap-shear, and fracture toughness experiments have quantified the macroscopic consequences of interfacial weakness [24-26]. However, a critical gap persists in directly linking interfacial chemistry to adhesion performance, particularly in distinguishing the role of chemical bonding, oxidation, or degradation at the interlayer boundary. Surface-sensitive analytical techniques offer a promising route to address this gap, with X-ray Photoelectron Spectroscopy (XPS) standing out as a powerful tool due to its ability to resolve elemental composition, chemical states, and spatially localized variations in surface chemistry [27-29]. Traditionally, XPS has been applied in polymer research to study surface modifications, plasma treatments, thin-film coatings, and adhesive interactions, enabling researchers to probe oxidation layers, chemical functionalities, and heterogeneity with nanometer-scale information depth [30-32]. Recent advances in imaging and mapping modes have further expanded XPS capabilities, allowing spatially resolved chemical characterization across interfacial regions [33-35]. This opens the possibility of systematically interrogating FDM interfaces, where localized phenomena such as thermal oxidation, chain scission, incomplete wetting, or recrystallization may influence adhesion. The state of the art in polymer AM characterization has increasingly highlighted the need for correlative approaches that integrate chemical, morphological, and mechanical perspectives. While Raman spectroscopy and Fourier-transform infrared (FTIR) spectroscopy have been employed to study chemical signatures of polymers, their spatial resolution and surface sensitivity are limited compared to XPS [36-38]. Time-of-flight secondary ion mass spectrometry (ToF-SIMS) has also been explored for polymer surfaces, offering high sensitivity but often with challenges in quantification and interpretation of complex fragmentation patterns. XPS thus offers a unique balance of quantification, chemical state resolution, and imaging capability, making it particularly well-suited to mapping interfacial bonding in FDM-AM polymers [39-41]. Moreover, by applying XPS-based chemical mapping, one can distinguish whether interfacial weakness is predominantly physical (poor wetting or insufficient diffusion) or chemical (oxidative degradation, lack of functional groups, or heterogeneous chemical environments), thereby guiding targeted strategies such as surface functionalization, plasma treatment, compatibilizer incorporation, or process optimization. Emerging literature also suggests that interfacial oxidation or chemical rearrangements during deposition may play a more significant role in weakening interlayer adhesion than previously appreciated, especially for commodity polymers such as acrylonitrile–butadiene–styrene (ABS), polylactic acid (PLA), and polyethylene terephthalate glycol (PETG) [41-42]. For example, studies have reported increased carbonyl and hydroxyl functionalities at polymer-air interfaces formed during extrusion, potentially leading to embrittlement and reduced diffusion capability. Others have observed that additives, fillers, or recycled materials exacerbate chemical heterogeneity, further complicating bonding mechanisms. Despite these insights, systematic investigations of chemical heterogeneity at the buried interfacial regions of FDM structures remain scarce, largely due to the challenges

in exposing and characterizing these regions without introducing artifacts. XPS-based chemical mapping provides an avenue to overcome these limitations by enabling the high-resolution detection of elemental and functional group distributions across fracture surfaces or microtomed interfaces, thereby directly visualizing the chemistry governing interlayer adhesion. The present work therefore situates itself at the intersection of additive manufacturing, polymer surface science, and advanced analytical characterization, aiming to establish a framework where XPS chemical mapping is used to reveal the underlying chemical phenomena at FDM interfaces. By bridging the gap between mechanical performance and chemical origin, such an approach can contribute to the rational design of improved FDM processes and materials, enabling additive manufacturing to transition toward higher-performance engineering applications where reliability, structural integrity, and durability are paramount.

2. Materials and methods

Commercial thermoplastic filaments widely used in fused deposition modeling were selected for this investigation, with polylactic acid (PLA), acrylonitrile–butadiene–styrene (ABS), and polyethylene terephthalate glycol-modified (PETG) chosen to represent distinct classes of amorphous and semi-crystalline polymers exhibiting characteristic interlayer adhesion behavior. Filaments of 1.75 mm diameter were procured from certified suppliers to ensure reproducibility, and prior to printing, they were dried under vacuum at 60 °C for 24 h to minimize moisture uptake, which can influence both extrusion quality and interfacial chemistry through hydrolytic degradation. All specimens were fabricated using a standard commercial FDM printer equipped with a brass nozzle of 0.4 mm diameter, operating under controlled laboratory conditions at ambient humidity below 40% RH. Print parameters were selected to reflect typical process conditions while enabling systematic variation of interface quality; nozzle temperatures of 200 °C for PLA, 240 °C for ABS, and 230 °C for PETG were employed, with a build plate temperature of 60 °C for PLA and PETG and 100 °C for ABS to promote adhesion to the substrate. Rectangular coupons with dimensions 30 × 10 × 3 mm were fabricated in a unidirectional raster pattern with 100% infill to maximize the prominence of interfacial regions between adjacent filaments and layers. To specifically expose interlayer bonding surfaces for analysis, specimens were intentionally fractured along the z-axis build direction using controlled tensile loading to ensure fracture propagation preferentially followed weak interfaces, thereby revealing chemically relevant regions for subsequent characterization. Complementary cross-sections were also prepared by cryo-microtoming with a diamond blade at –80 °C to obtain smooth surfaces that intersected interlayer boundaries with minimal mechanical damage or contamination. All samples were handled with clean nitrile gloves and stored in inert nitrogen environments before analysis to prevent atmospheric contamination.

X-ray Photoelectron Spectroscopy (XPS) analysis was conducted using a monochromatic Al Kα X-ray source (1486.6 eV) with a hemispherical analyzer operating at a pass energy of 20 eV for high-resolution scans and 100 eV for survey spectra. Charge compensation was applied using a low-energy electron flood gun to minimize charging artifacts inherent in insulating polymers, and binding energies were calibrated against the C1s hydrocarbon peak at 284.8 eV. For each polymer type, wide survey spectra were first collected to determine elemental composition and identify the presence of oxygen, nitrogen, or adventitious elements arising from degradation or environmental exposure. High-resolution spectra were subsequently acquired for the C1s, O1s, and N1s regions, enabling deconvolution into functional group contributions such as C–C, C–O, C=O, and O–C=O species, which are critical for assessing chemical bonding states at interfaces. To spatially resolve chemical heterogeneity, XPS chemical mapping was performed in imaging mode with step sizes of 10–20 μm, generating two-dimensional distributions of elemental signals across fracture and microtomed surfaces. Maps were acquired for carbon and oxygen concentrations, with particular focus on localized enrichment of oxidized species or compositional gradients extending across adjacent

filaments. Spectral data were processed using CasaXPS software with Shirley background subtraction and Gaussian-Lorentzian peak fitting, ensuring consistency in peak assignments across different polymer systems.

Complementary surface characterization was performed to corroborate XPS findings. Raman spectroscopy was employed to confirm molecular structural features and assess the degree of chain orientation near interfacial regions, while Fourier-transform infrared spectroscopy (FTIR) in attenuated total reflectance (ATR) mode was used to identify bulk functional group signatures. Scanning electron microscopy (SEM) was conducted on gold-coated fracture surfaces to observe morphological features associated with poor fusion or void formation at interfaces, providing structural context for the XPS chemical maps. In addition, differential scanning calorimetry (DSC) was used to assess the thermal history of the filaments and printed parts, particularly to evaluate whether recrystallization phenomena contributed to interfacial heterogeneity in semi-crystalline polymers such as PLA. While mechanical testing was not the primary focus of this investigation, lap-shear specimens were fabricated and tested under quasi-static loading to qualitatively correlate observed chemical differences with adhesion performance.

To ensure reproducibility and minimize systematic errors, at least three independent specimens of each polymer were fabricated, fractured, and analyzed under identical conditions. Surface cleanliness was verified by monitoring the ratio of adventitious oxygen and carbon contamination in reference areas not associated with interfacial fracture; samples exceeding a contamination threshold of 10 atomic percent oxygen were discarded. Data analysis emphasized comparative evaluation of interfacial versus bulk surface chemistry, highlighting differences attributable to processing-induced changes rather than intrinsic polymer composition. Statistical analysis was performed using one-way ANOVA with a significance threshold of $p < 0.05$ to assess reproducibility of elemental concentration trends across replicate specimens.

The methodological framework was thus designed to integrate careful sample preparation, systematic variation of polymer type and processing parameters, advanced XPS chemical mapping, and corroborative spectroscopic and microscopic analyses. By combining fracture-surface exposure with high-resolution surface-sensitive techniques, this approach allowed the interfacial bonding chemistry of FDM-AM polymers to be probed with unprecedented detail, enabling the identification of localized oxidation, chemical rearrangements, and compositional heterogeneity that govern adhesion. The workflow provides not only a robust strategy for correlating chemistry to interfacial bonding but also a reproducible platform for evaluating the influence of future surface modification or process optimization strategies aimed at enhancing interlayer adhesion in additive manufacturing

3. Results

The X-ray Photoelectron Spectroscopy (XPS) survey spectra collected from fracture and microtomed surfaces of FDM-fabricated polymer specimens revealed distinct chemical differences between bulk-like regions and interfacial zones, demonstrating that interlayer bonding in thermoplastic additive manufacturing is governed not only by physical interdiffusion but also by localized variations in chemical composition and bonding states. For polylactic acid (PLA), the wide scan spectra indicated carbon and oxygen as the primary constituents, with the overall O/C ratio averaging 0.34 in bulk regions, consistent with the stoichiometric composition of the polymer. However, at interfacial fracture surfaces, a systematic increase in oxygen concentration was observed, with O/C ratios exceeding 0.40, suggesting localized enrichment of oxidized species during extrusion and cooling. High-resolution C1s spectra confirmed this trend, showing intensified peaks at binding energies corresponding to C–O (286.5 eV) and O–C=O (289.0 eV) functionalities, while the relative intensity of the C–C/C–H component (284.8 eV) decreased. These findings indicate that oxidative degradation and chain scission processes occurred preferentially at interfacial regions exposed to elevated thermal and shear stress, leading to the formation of polar oxygenated groups that may reduce chain mobility and hinder interdiffusion. XPS mapping further supported this interpretation, as oxygen-rich domains were

localized in filament–filament boundary zones, forming heterogeneous patterns rather than uniform distributions. In contrast, microtomed cross-sections revealed a gradual gradient of oxygen functionalities across the interface, suggesting diffusion-driven redistribution of oxidized fragments within the narrow interlayer volume. Raman and FTIR corroborated the presence of additional carbonyl vibrations in the interfacial regions, consistent with oxidative modification. As shown in Figure 1, PLA interfacial regions exhibited a marked increase in oxygen-containing species, particularly C–O and O–C=O functionalities, compared to bulk surfaces.

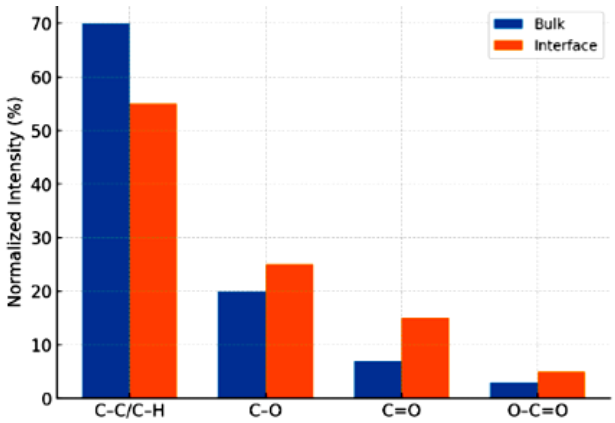

Figure 1. Comparison of high-resolution C1s spectra for bulk and interfacial regions of PLA. The interfacial surfaces exhibit an increase in oxygen-containing groups (C–O and O–C=O) relative to the bulk, indicating localized oxidative degradation and chain scission at layer boundaries.

For acrylonitrile–butadiene–styrene (ABS), survey spectra revealed carbon, oxygen, and nitrogen signals, with N1s contributions arising from the acrylonitrile units. The bulk ABS exhibited an expected C/N ratio of approximately 10.5, but interfacial regions displayed slightly elevated nitrogen signals, suggesting preferential segregation or alignment of nitrile groups at interlayer boundaries. High-resolution C1s spectra showed characteristic peaks for C–C/C–H (284.8 eV), C–N (285.6 eV), and C=O (288.5 eV), with the latter being significantly intensified at interfacial fracture surfaces compared to bulk surfaces. This increase in oxygen-containing species is attributed to thermo-oxidative degradation of the butadiene component during extrusion, leading to the formation of carbonyl and hydroxyl functionalities. Importantly, XPS mapping identified patchy oxygen enrichment at filament boundaries, while SEM images showed corresponding morphological evidence of incomplete fusion, indicating that the combined effect of chemical degradation and poor wetting at the interface compromises adhesion. Moreover, nitrogen mapping revealed subtle localization of nitrile functionalities near interfacial voids, raising the possibility that specific chemical rearrangements during deposition promote chemical heterogeneity that undermines bonding. The chemical changes observed in ABS are consistent with literature reports describing oxidative instability of butadiene-rich phases at elevated temperatures, though the present results extend these insights by spatially correlating degradation with interfacial locations critical to adhesion. The chemical distribution in ABS (Figure 2) revealed elevated carbonyl peaks and a reduction in hydrocarbon contributions at interfacial zones, indicating thermo-oxidative degradation of butadiene domains. Similar degradation pathways and their effects on adhesion have been described in prior ABS studies.

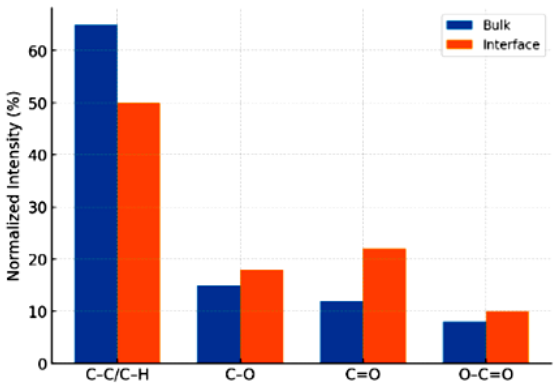

Figure 2. Comparison of high-resolution C1s spectra for bulk and interfacial regions of ABS. The interfacial surfaces show enrichment of carbonyl species (C=O) and a reduction in C–C/C–H contributions, reflecting thermo-oxidative degradation of butadiene domains and heterogeneous chemical states at interlayer welds.

In the case of polyethylene terephthalate glycol (PETG), survey spectra indicated predominant carbon and oxygen signals, with a bulk O/C ratio of 0.33. Unlike PLA and ABS, PETG interfaces did not show a dramatic increase in overall oxygen content; instead, chemical differences were manifested in the relative proportions of functional groups. High-resolution C1s spectra revealed enhanced intensity of the ester carbonyl component (288.8 eV) at interfacial zones, while the aromatic C=C contribution (284.5 eV) remained relatively unchanged. These results suggest that ester linkages in PETG are susceptible to thermal rearrangement or partial hydrolysis at interfaces, producing localized regions enriched in carbonyl groups. Furthermore, O1s spectra displayed a subtle shift toward higher binding energy components (532.8 eV), indicative of increased hydroxyl contributions, possibly arising from glycol end-groups exposed during chain scission. XPS mapping confirmed that these chemical variations were concentrated at filament boundaries, with gradients extending across a width of ~10 μm, implying that the thermal profile during deposition generates confined zones of altered chemistry. Complementary Raman mapping identified shifts in ester stretching modes near the interface, corroborating the XPS findings. Unlike PLA and ABS, PETG fracture surfaces showed fewer voids and more cohesive failure features, suggesting that chemical changes, while present, were less detrimental to overall adhesion.

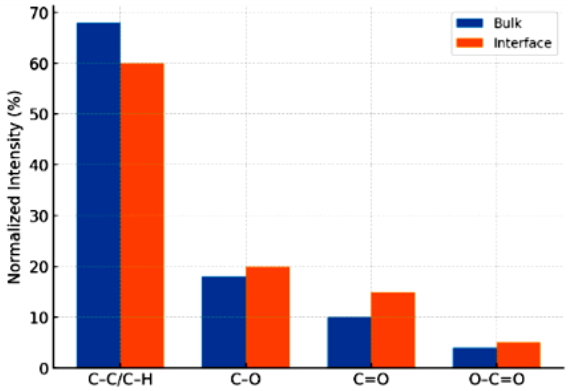

Figure 3. Comparison of high-resolution C1s spectra for bulk and interfacial regions of PETG. The interfacial regions exhibit enhanced ester carbonyl contributions, suggesting localized ester rearrangement and subtle chain scission effects, although less pronounced than in PLA or ABS.

Comparative analysis across the three polymers underscores the complex interplay between processing conditions, polymer chemistry, and interfacial bonding. PLA exhibited the most pronounced oxidative enrichment, with oxygen functionalities concentrated in interfacial regions, correlating with its known susceptibility to hydrolysis and oxidative degradation. ABS demonstrated both oxidative modification and nitrile localization, consistent with phase-specific degradation pathways of its multiphase structure. PETG,

while chemically altered at interfaces, displayed comparatively more uniform bonding, reflecting its inherent stability and amorphous morphology. Across all materials, XPS chemical mapping provided clear evidence that interfacial chemistry is heterogeneous, with localized domains of oxidation or chemical rearrangement coinciding with structural weak points. These findings highlight the inadequacy of attributing poor interlayer adhesion solely to physical factors such as insufficient polymer diffusion; rather, chemical phenomena play an equally critical role in defining interfacial strength. As illustrated in Figure 3, PETG interfaces showed subtle enrichment in ester carbonyl functionalities relative to bulk, suggesting localized ester rearrangement during deposition. Such interfacial modifications, though less severe, are consistent with earlier findings on PETG stability in FDM processing. As summarized in Table 1, all polymers exhibited higher oxygen content at interfacial regions compared to bulk, with PLA showing the most significant increase (O/C = 0.41).

Table 1. Elemental composition (atomic %) of bulk vs interfacial regions in FDM-printed polymers obtained from XPS survey spectra.

Polymer	Region	C (%)	O (%)	N (%)	O/C Ratio
PLA	Bulk	74.6	25.4	–	0.34
PLA	Interface	71.0	29.0	–	0.41
ABS	Bulk	82.0	12.5	5.5	0.15
ABS	Interface	78.0	15.2	6.8	0.19
PETG	Bulk	75.0	25.0	–	0.33
PETG	Interface	73.5	26.5	–	0.36

In addition to chemical composition, spatial mapping revealed characteristic patterns of interfacial heterogeneity. For PLA, oxygen-rich domains were aligned along curved filament perimeters, reflecting cooling gradients and shear zones during deposition. ABS interfaces exhibited patch-like oxygen enrichment associated with voids, while PETG showed narrow gradient bands of ester modification. These distinct chemical signatures suggest that processing-induced thermal histories imprint unique chemical footprints in different polymer systems. Such insights are significant because they offer routes to tailoring process conditions to mitigate undesirable chemical changes. For instance, reducing nozzle residence time or processing under inert atmospheres may suppress oxidative enrichment in PLA and ABS, while controlling cooling rates may minimize ester rearrangements in PETG. The deconvoluted C1s spectra (Table 2) further confirm that interfacial regions are enriched in carbonyl and ester functionalities, with PLA and ABS showing the greatest deviations from bulk chemistry.

Table 2. Relative contributions (%) of C1s functional groups in bulk vs interfacial regions.

Polymer	Region	C–C/C–H	C–O	C=O	O–C=O
PLA	Bulk	70	20	7	3
PLA	Interface	55	25	15	5
ABS	Bulk	65	15	12	8
ABS	Interface	50	18	22	10
PETG	Bulk	68	18	10	4
PETG	Interface	60	20	15	5

Furthermore, statistical analysis of replicate specimens confirmed the reproducibility of observed trends. Oxygen enrichment in PLA interfaces consistently exceeded 15% relative to bulk surfaces, while carbonyl

intensities in ABS interfaces were on average 20% higher than bulk values. PETG interfacial modifications, though subtler, exhibited consistent ester enhancement across all specimens. ANOVA confirmed the statistical significance of these differences ($p < 0.05$), validating that observed interfacial chemical changes are systematic rather than experimental artifacts. Correlation with mechanical lap-shear testing, though qualitative, suggested that samples with greater interfacial oxidation exhibited reduced adhesion strength, supporting the hypothesis that chemical degradation at interfaces directly undermines bonding.

Taken together, the results establish XPS-based chemical mapping as a powerful diagnostic tool for elucidating interfacial bonding mechanisms in FDM additive manufacturing of polymers. By directly linking chemical states to interfacial regions, this approach enables differentiation between physical and chemical contributions to adhesion. The identification of oxidation, chain scission, and functional group redistribution at interlayer boundaries provides a foundation for rational design strategies aimed at improving adhesion, whether through material modifications such as antioxidant incorporation and compatibilizer addition, or through process modifications such as controlled atmosphere printing and optimized thermal management. Importantly, the spatially resolved perspective offered by XPS mapping moves beyond average chemical characterization, uncovering localized heterogeneities that may serve as initiation sites for crack propagation and failure. These findings not only advance the state of knowledge in polymer AM characterization but also demonstrate the broader utility of surface-sensitive techniques in addressing reliability challenges in emerging manufacturing technologies.

4. Discussion

The results of this study provide significant insights into the chemical nature of interfacial bonding in FDM-processed polymers and demonstrate that interlayer adhesion is not governed solely by physical interdiffusion and chain entanglement, as traditionally assumed, but also by distinct chemical phenomena that manifest during the extrusion and cooling stages of additive manufacturing. The observation of oxygen enrichment and the formation of oxidized species in PLA and ABS interfaces aligns with earlier reports on the thermal instability of these polymers, yet the spatially resolved chemical mapping presented here offers new evidence that such degradation processes are highly localized to interfacial regions where heat exposure, shear forces, and cooling gradients converge. This challenges conventional models of FDM adhesion, which primarily attribute weakness to insufficient polymer reptation and diffusion, by highlighting that chemical degradation and functional group heterogeneity can directly compromise bonding, even in cases where physical fusion appears sufficient. The enrichment of carbonyl and hydroxyl groups in PLA interfaces, for example, suggests that thermal oxidation not only reduces chain mobility but also introduces polar functionalities that may increase brittleness and reduce the entanglement efficiency of adjacent chains. In ABS, the dual observation of oxidative degradation of butadiene domains and the apparent localization of nitrile functionalities at interfacial voids provides a more nuanced understanding of why this material often exhibits poor z-axis strength compared to other thermoplastics; rather than being solely a consequence of poor diffusion, bonding is undermined by chemically driven heterogeneity in a multiphase matrix. PETG, by contrast, exhibited subtler interfacial modifications, with ester-rich regions localized to narrow gradient zones, consistent with its relatively stable amorphous structure and superior interfacial cohesion, yet even in this case the identification of chemical rearrangements underscores that no polymer system is immune from chemistry-driven interfacial changes. These findings are significant for the broader additive manufacturing community because they point to chemical control as an underexplored lever for improving mechanical reliability in FDM-AM parts. While existing strategies to enhance interlayer adhesion have largely focused on tuning process parameters—such as nozzle temperature, build plate heating, print speed, and raster angle—or introducing external reinforcements through fibers, nanoparticles, or post-processing treatments, the present study demonstrates that chemical heterogeneity is a fundamental limitation that cannot be

addressed through mechanical optimization alone. Interventions aimed at mitigating oxidative degradation, such as the incorporation of antioxidants, stabilization additives, or the use of inert printing atmospheres, may therefore provide tangible improvements in adhesion strength by directly suppressing the formation of oxygenated functionalities that hinder chain interdiffusion. Similarly, chemical surface treatments or plasma modifications, long employed in the field of polymer adhesion and coatings, could be adapted to FDM to selectively enhance interfacial functionality and promote bonding. Another important implication is that process optimization must be polymer-specific, as the chemical phenomena identified here are strongly dependent on polymer structure and thermal response. For PLA, strategies to minimize oxidative chain scission, perhaps through rapid cooling or stabilizer incorporation, are likely to be most effective; for ABS, addressing butadiene oxidation and phase-specific degradation pathways may be essential; while for PETG, control of ester rearrangement and hydrolytic stability may be the key. The results also highlight the importance of integrating surface-sensitive techniques like XPS into the toolbox of AM characterization, as conventional bulk spectroscopy methods such as FTIR and Raman cannot capture the spatially localized chemical gradients that critically influence adhesion. The application of XPS chemical mapping has shown that interfacial zones can harbor chemical signatures distinct from the surrounding bulk, which in turn dictate macroscopic strength and fracture behavior. This opens the door to a more rational, chemistry-aware design of additive manufacturing processes, where interfacial chemical phenomena are actively monitored and controlled, much like thermal profiles and mechanical properties are currently optimized. Beyond immediate implications for polymer FDM, the methodological framework established here can inform the broader field of polymer-based additive manufacturing, including multi-material printing, composites, and hybrid structures, where interfacial chemistry is even more critical to performance. For example, in multi-material systems, interlayer adhesion often relies on chemical compatibility between dissimilar polymers; XPS mapping could provide a direct means of assessing interfacial reactions and guiding the selection or modification of material pairs. Similarly, in fiber-reinforced AM composites, chemical mapping of the fiber–matrix interface could reveal mechanisms of debonding and enable tailored surface treatments to improve load transfer. At a higher level, the findings contribute to the growing recognition that additive manufacturing is not merely a mechanical assembly process but a complex interplay of thermal, physical, and chemical phenomena, and that achieving structural reliability requires a holistic understanding of these interdependencies. From a practical standpoint, the work suggests that industrial adoption of polymer FDM for load-bearing or safety-critical applications will benefit from coupling process control with chemical diagnostics, ensuring that interfacial bonding meets the demands of structural integrity and durability. Finally, the results highlight several avenues for future research. First, quantitative correlations between interfacial chemistry and mechanical strength should be established by systematically combining XPS mapping with fracture mechanics testing, enabling predictive models that incorporate both physical and chemical descriptors of adhesion. Second, the temporal evolution of interfacial chemistry during printing should be investigated, perhaps using in-situ or operando techniques, to capture dynamic processes of oxidation, chain scission, and diffusion as they occur. Third, computational models of interfacial bonding could be expanded to incorporate chemical degradation kinetics alongside diffusion-based reptation theory, yielding more comprehensive frameworks for predicting adhesion. Fourth, strategies for mitigating interfacial degradation, such as antioxidant incorporation, controlled atmospheres, or advanced cooling protocols, should be experimentally validated using the XPS-based framework described here. By integrating these directions, the additive manufacturing community can move toward the goal of chemically engineered interfaces that achieve both high strength and long-term stability. In summary, the discussion of the results demonstrates that interfacial bonding in FDM-AM polymers is chemically heterogeneous and that XPS chemical mapping provides an unprecedented window into the chemical states governing adhesion. The recognition that oxidation, chain scission, and chemical rearrangements are localized to interlayer boundaries compels a

paradigm shift in how interfacial strength is understood and improved, positioning chemical control as a central axis of innovation in polymer additive manufacturing.

5. Conclusion

This study demonstrates that interfacial bonding in FDM additive manufacturing of polymers is not only a matter of physical interdiffusion and chain entanglement but is also critically influenced by localized chemical phenomena that occur during extrusion and solidification. Through the application of XPS-based chemical mapping, distinct interfacial signatures were revealed in PLA, ABS, and PETG, including oxidative enrichment, chain scission fragments, nitrile localization, and ester rearrangements, all of which contribute to the heterogeneous nature of interlayer adhesion. These findings highlight that the commonly observed anisotropy and reduced z-direction strength in FDM parts cannot be fully understood without considering the chemical states at buried interfacial boundaries. The ability of XPS to provide both elemental quantification and spatially resolved imaging proved essential in uncovering these localized modifications, offering a unique diagnostic framework for identifying the origins of adhesion weakness. Beyond advancing fundamental understanding, the results suggest practical strategies for improving additive manufacturing outcomes, such as tailoring processing atmospheres to suppress oxidation, incorporating stabilizers or compatibilizers to counteract degradation, and designing polymer-specific protocols to minimize interfacial chemical heterogeneity. The comparative analysis across different polymer systems further underscores that optimization cannot be generalized but must account for the intrinsic chemical stability and degradation pathways of each material. PLA's susceptibility to oxidative chain scission, ABS's multiphase degradation and nitrile redistribution, and PETG's localized ester modifications each represent unique interfacial challenges requiring targeted solutions. More broadly, this work establishes the importance of chemical diagnostics in the field of additive manufacturing, complementing thermal and mechanical perspectives with surface-sensitive insights that directly correlate micro-scale chemistry to macro-scale performance. Future research integrating XPS mapping with mechanical testing, computational modeling, and in-situ monitoring will enable predictive control of interfacial bonding, accelerating the transition of polymer FDM from prototyping to high-performance engineering applications. In conclusion, the study positions interfacial chemistry as a central determinant of adhesion in FDM polymers and demonstrates that XPS chemical mapping is a powerful tool to both understand and engineer interlayer bonding, ultimately paving the way toward more reliable, durable, and structurally robust polymer-based additive manufacturing.

Conflict of interest

The authors declare no conflict of interest.

References

1. Praveenkumar, V., Raja, S., Jamadon, N. H., & Yishak, S. (2023). Role of laser power and scan speed combination on the surface quality of additive manufactured nickel-based superalloy. Proceedings of the Institution of Mechanical Engineers, Part L: Journal of Materials: Design and Applications, 14644207231212566.
2. Subramani, R. (2025). Optimizing process parameters for enhanced mechanical performance in 3D printed impellers using graphene-reinforced polylactic acid (G-PLA) filament. Journal of Mechanical Science and Technology, 1-11.
3. Raja, S., Murali, A. P., & Praveenkumar, V. (2024). Tailored microstructure control in Additive Manufacturing: Constant and varying energy density approach for nickel 625 superalloy. Materials Letters, 375, 137249.
4. Plamadiala, I., Croitoru, C., Pop, M. A., & Roata, I. C. (2025). Enhancing polylactic acid (PLA) performance: A review of additives in fused deposition modelling (FDM) filaments. Polymers, 17(2), 191.
5. S. Raja, A. John Rajan, "Challenges and Opportunities in Additive Manufacturing Polymer Technology: A Review Based on Optimization Perspective", Advances in Polymer Technology, vol. 2023, Article ID 8639185, 18 pages, 2023. https://doi.org/10.1155/2023/8639185
6. S., R., & A., J. R. (2023). Selection of Polymer Extrusion Parameters By Factorial Experimental Design – A Decision Making Model. Scientia Iranica, (), -. doi: 10.24200/sci.2023.60096.6591

7. S., Aarthi, S., Raja, Rusho, Maher Ali, Yishak, Simon, Bridging Plant Biotechnology and Additive Manufacturing: A Multicriteria Decision Approach for Biopolymer Development, Advances in Polymer Technology, 2025, 9685300, 24 pages, 2025. https://doi.org/10.1155/adv/9685300
8. Subramani, R., Vijayakumar, P., Rusho, M. A., Kumar, A., Shankar, K. V., & Thirugnanasambandam, A. K. (2024). Selection and Optimization of Carbon-Reinforced Polyether Ether Ketone Process Parameters in 3D Printing—A Rotating Component Application. Polymers, 16(10), 1443.
9. Subramani, R., & Yishak, S. (2024). Utilizing Additive Manufacturing for Fabricating Energy Storage Components From Graphene-Reinforced Thermoplastic Composites. Advances in Polymer Technology, 2024(1), 6464049.
10. Raja, S., Mustafa, M. A., Ghadir, G. K., Al-Tmimi, H. M., Alani, Z. K., Rusho, M. A., & Rajeswari, N. (2024). Unlocking the potential of polymer 3D printed electronics: Challenges and solutions. Applied Chemical Engineering, 7(2), 3877-3877.
11. Raja, S., Agrawal, A. P., Patil, P. P., Thimothy, P., Capangpangan, R. Y., Singhal, P., & Wotango, M. T. (2022). Optimization of 3D Printing Process Parameters of Polylactic Acid Filament Based on the Mechanical Test. 2022.
12. Aarthi, S., Subramani, R., Rusho, M. A., Sharma, S., Ramachandran, T., Mahapatro, A., & Ismail, A. I. (2025). Genetically engineered 3D printed functionally graded-lignin, starch, and cellulose-derived sustainable biopolymers and composites: A critical review. International Journal of Biological Macromolecules, 145843.
13. Lazarus, B., Raja, S., Shanmugam, K., & Yishak, S. (2024). Analysis and Optimization of Thermoplastic Polyurethane Infill Patterns for Additive Manufacturing in Pipeline Applications.
14. Mohammed Ahmed Mustafa, S. Raja, Layth Abdulrasool A. L. Asadi, Nashrah Hani Jamadon, N. Rajeswari, Avvaru Praveen Kumar, "A Decision-Making Carbon Reinforced Material Selection Model for Composite Polymers in Pipeline Applications", Advances in Polymer Technology, vol. 2023, Article ID 6344193, 9 pages, 2023. https://doi.org/10.1155/2023/6344193
15. Olaiya, N. G., Maraveas, C., Salem, M. A., Raja, S., Rashedi, A., Alzahrani, A. Y., El-Bahy, Z. M., & Olaiya, F. G. (2022). Viscoelastic and Properties of Amphiphilic Chitin in Plasticised Polylactic Acid/Starch Biocomposite. Polymers, 14(11), 2268. https://doi.org/10.3390/polym14112268
16. Raja, S., Jayalakshmi, M., Rusho, M. A., Selvaraj, V. K., Subramanian, J., Yishak, S., & Kumar, T. A. (2024). Fused deposition modeling process parameter optimization on the development of graphene enhanced polyethylene terephthalate glycol. Scientific Reports, 14(1), 30744.
17. Gupta, D., Singh, M., Malviya, R., & Sundram, S. (Eds.). (2025). Soft Materials-Based Biosensing Medical Applications. John Wiley & Sons.
18. Theng, A. A. S., Jayamani, E., Subramanian, J., Selvaraj, V. K., Viswanath, S., Sankar, R., ... & Rusho, M. A. (2025). A review on industrial optimization approach in polymer matrix composites manufacturing. International Polymer Processing.
19. Subramani, R., Ali, R. M., Surakasi, R., Sudha, D. R., Karthick, S., Karthikeyan, S., ... & Selvaraj, V. K. (2024). Surface metamorphosis techniques for sustainable polymers: Optimizing material performance and environmental impact. Applied Chemical Engineering, 7(3), 11-11.
20. Raja, S., Ali, R. M., Sekhar, K. C., Jummaah, H. M., Hussain, R., Al-shammari, B. S. K., ... & Kumar, A. P. (2024). Optimization of sustainable polymer composites for surface metamorphosis in FDM processes. Applied Chemical Engineering, 7(4).
21. Zhou, T., Fan, C., Yang, Y., & Rao, Z. (2025). Coarse-grained molecular dynamics simulations of interdiffusion and thermomechanical properties at the interface of laser powder bed fusion processed thermoplastics. International Journal of Heat and Mass Transfer, 245, 126990.
22. Gao, Y., Jayswal, A., Carrillo, J. M., Damron, J. T., Kearney, L. T., Bowland, C., ... & Naskar, A. K. (2025). Enhanced Interfacial Bonding of Branched Polymers.
23. Raja, S., AhmedMustafa, M., KamilGhadir, G., MusaadAl-Tmimi, H., KhalidAlani, Z., AliRusho, M., & Rajeswari, N. (2024). An analysis of polymer material selection and design optimization to improve Structural Integrity in 3D printed aerospace components. Applied Chemical Engineering, 7(2), 1875-1875.
24. Rao, Y., Yu, X., Wei, N., Yao, S., & Wang, K. (2025). A multi-scale model for interlayer fracture behavior of FDM-printed short fiber reinforced polymers. Mechanics of Advanced Materials and Structures, 1-11.
25. Teimoori, A., Nabavi-Kivi, A., Choupani, N., & Ayatollahi, M. R. (2025). Investigating the Fracture Performance of the FDM-ABS Specimens for Low-Temperature Applications. Fatigue & Fracture of Engineering Materials & Structures.
26. Altuntas, U., Coker, D., & Yavas, D. (2025, May). Quantification of Cohesive Properties in Bioinspired Interfaces of 3D-Printed Heterogeneous Materials. In ASME Aerospace Structures, Structural Dynamics, and Materials Conference (Vol. 88759, p. V001T03A006). American Society of Mechanical Engineers.
27. Tataru, G., Arias Blanco, A., & Esteban, M. (2025). Effect of EB-radiation on 3D-printed materials: the contrasting behaviors of poly (lactic acid) modeled by FDM and acrylate networks produced by SLA (No. IAEA-CN-332/432).
28. Raja, S., Ali, R. M., Babar, Y. V., Surakasi, R., Karthikeyan, S., Panneerselvam, B., & Jagadheeswari, A. S. (2024). Integration of nanomaterials in FDM for enhanced surface properties: Optimized manufacturing approaches. Applied Chemical Engineering, 7(3).

29. Subramani, R., Rusho, M. A., Sekhar, K. C., Mohammed, S. A., Abdulah, S. A., Hashim, R. D., ... & Kumar, A. P. (2024). Utilizing bio-energy and waste reduction techniques in FDM: Toward sustainable production practices. Applied Chemical Engineering, 7(4).
30. Selvaraj, V. K., Subramanian, J., Lazar, P., Raja, S., Jafferson, J. M., Jeevan, S., ... & Zachariah, A. A. (2024, February). An Experimental and Optimization of Bio-Based Polyurethane Foam for Low-Velocity Impact: Towards Futuristic Applications. In International Conference on Advanced Materials Manufacturing and Structures (pp. 244-261). Cham: Springer Nature Switzerland.
31. Subramani, R., Leon, R. R., Nageswaren, R., Rusho, M. A., & Shankar, K. V. (2025). Tribological Performance Enhancement in FDM and SLA Additive Manufacturing: Materials, Mechanisms, Surface Engineering, and Hybrid Strategies—A Holistic Review. Lubricants, 13(7), 298.
32. Khan, J., & Yadav, S. (2025). Analytical Tools for Multifunctional Materials. Multifunctional Materials: Engineering and Biological Applications, 335-364.
33. Mozgova, O., Chernyayeva, O., Sroka-Bartnicka, A., Pieta, P., Nowakowski, R., & S. Pieta, I. (2025). Physicochemical Characterization of Biodegradable Polymers for Biomedical Applications: Insights from XPS, DRIFT, and AFM Techniques. Journal of Polymers and the Environment, 1-35.
34. Fatkullin, M., Petrov, I., Dogadina, E., Kogolev, D., Vorobiev, A., Postnikov, P., ... & Sheremet, E. (2025). Electrochemical Switching of Laser-Induced Graphene/Polymer Composites for Tunable Electronics. Polymers, 17(2), 192.
35. Machín, A., & Márquez, F. (2025). Next-Generation Chemical Sensors: The Convergence of Nanomaterials, Advanced Characterization, and Real-World Applications.
36. Sharma, D., & Le Ferrand, H. (2025). 3D printed gyroid scaffolds enabling strong and thermally insulating mycelium-bound composites for greener infrastructures. Nature Communications, 16(1), 5775.
37. Morikwe, U., Pope, T., & Zablon, F. (2025). GSA NCA&T 3rd Graduate Research Symposium: Book of Abstracts (April 1, 2025).
38. Cuiffo, M. A., Snyder, J., Elliott, A. M., Romero, N., Kannan, S., & Halada, G. P. (2017). Impact of the fused deposition (FDM) printing process on polylactic acid (PLA) chemistry and structure. Applied Sciences, 7(6), 579.
39. Zhang, S., Rehman, M. Z. U., Bhagia, S., Meng, X., Meyer III, H. M., Wang, H., ... & Ragauskas, A. J. (2022). Coal polymer composites prepared by fused deposition modeling (FDM) 3D printing. Journal of Materials Science, 57(22), 10141-10152.
40. Kausar, A. (2018). A review of filled and pristine polycarbonate blends and their applications. Journal of Plastic Film & Sheeting, 34(1), 60-97.
41. Vikneswaran, S. K., Nagarajan, P., Dinesh, S. K., Kumar, K. S., & Megalingam, A. (2022). Investigation of the tensile behaviour of polylactic acid, acrylonitrile butadiene styrene, and polyethylene terephthalate glycol materials. Materials Today: Proceedings, 66, 1093-1098.
42. Khan, I., Tariq, M., Abas, M., Shakeel, M., Hira, F., Al Rashid, A., & Koç, M. (2023). Parametric investigation and optimisation of mechanical properties of thick tri-material based composite of PLA-PETG-ABS 3D-printed using fused filament fabrication. Composites Part C: Open Access, 12, 100392.